Journal of Alloys and Compounds, 195 (1993) 101–104
JALCOM 7424

Microstructural studies of non-stoichiometric YBCO thick films processed on YSZ substrates

T.J. Gray, T.C. Shields, F. Wellhofer and J.S. Abell

School of Metallurgy & Materials, The University of Birmingham, Birmingham. B15 2TT. UK.

Abstract

In order to improve the performance of superconducting YBCO thick films and control the properties it is imperative to gain a better understanding of the microstructural characteristics. Thick films produced from different non-stoichiometric YBCO compositions were screen-printed onto YSZ substrates and heat treated above Tp. The microstructures and superconducting properties of these tracks have been systematically investigated. Characterisation of the precursor materials and films were carried out by XRD. Optical and electron microscopy, EDX and electrical measurements have also been used to perform detailed studies and assessments of the films. Microstructural observations and superconducting properties relating to these thick films are discussed in detail.

1. Introduction

YBCO thick films produced by screen printing techniques onto YSZ substrates have attractive properties for potential application in microelectronics and high frequency devices. We have already shown that the performance of thick films can be enhanced by partial melting introduced by use of processing temperatures above the peritectic temperature of YBCO [1 & 2]. However, the performance of the films is limited, partly due to the presence of multiple phases resulting from the reaction between the 123 and the YSZ substrate [3].

Crystal growth experiments have routinely employed a self-fluxing method with an excess of Ba and Cu cations [4-6]. By applying a similar use of excess material to the precursor powder used to produce thick films it is shown that grain growth may also be enhanced in YBCO tracks. Flux additions also reduce the peritectic temperature therefore suggesting the potential for lowering the processing temperatures. This paper investigates the effects of various additions of excess Ba and Cu cations to YBCO thick films.

2. Experimental Procedure

YBCO powders were prepared from Y_2O_3, $BaCO_3$ and CuO reacted at 900°C for 36 hours in air with intermediate grinding stages. Non-stoichiometric powders of various compositions, achieved by additions of differing quantities of flux, were then produced following two different routes. The flux was produced by separately calcining mixtures of $BaCO_3$ and CuO (1) or $BaCuO_2$ and CuO (2). The flux was then added to the YBCO powder in the proportions A, B and C as shown in Fig. 1 and Table 1. All compositions were again precalcined at 900°C for 36 hours prior to preparation of the ink. The repeated calcining and regrinding steps were employed to achieve maximum homogeneity in the starting material. The powders were then assessed by XRD.

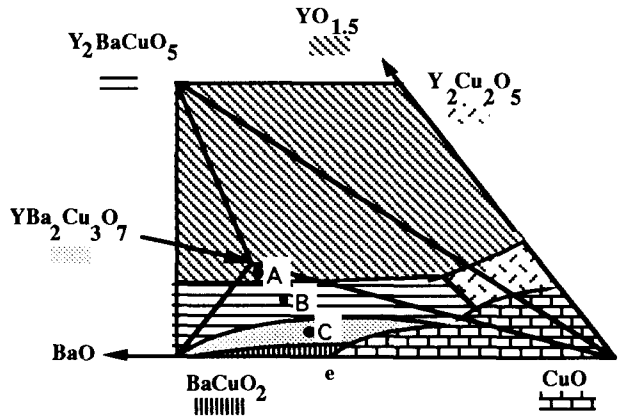

Fig . 1 Liquidus surface of the $YO_{1.5}$-BaO-CuO pseudo ternary phase diagram in air [7]. Work has been carried out using powders A (123 + 8.8% flux), B (123 + 32.4% flux) and C (123 + 64.7% flux) where the eutectic e represents 100% flux.

Sample	% Flux addition	Constituent powders	Ratio (Y:Ba:Cu)
Control	0.0	123	1 : 2 : 3
A(1)	8.8	123/$BaCO_3$/CuO	1 : 2.13 : 3.32
A(2)	8.8	123/$BaCuO_2$/CuO	1 : 2.13 : 3.32
B(1)	32.4	123/$BaCO_3$/CuO	1 : 2.87 : 5.87
B(2)	32.4	123/$BaCuO_2$/CuO	1 : 2.87 : 5.87
C(1)	64.7	123/$BaCO_3$/CuO	1 : 5.5 : 10.17
C(2)	64.7	123/$BaCuO_2$/CuO	1 : 5.5 : 10.17

Table 1. Table showing compositions of precursor powders

An YBCO control powder and the non-stoichiometric powders were each mixed with an industrial organic binder to produce an ink of the appropriate consistency for screen printing. Thick films were then produced by screen printing the inks onto YSZ substrates through a

0925-8388/93/$06.00

© 1993 – Elsevier Sequoia. All rights reserved

stainless steel screen with a simple 5mm x 25mm pattern. The thickness was controlled by multiple screen printing passes. The tracks were processed at 1035°C for 6 minutes in a flowing oxygen atmosphere to promote partial melting, with heating and cooling rates of 5°C/min and 2°C/min respectively. The track thicknesses after firing were approximately 40μm.

Characterisation of the tracks was performed using SEM and optical microscopy, A.C. susceptibility and resistivity measurement, XRD and D.C. critical current assessment.

3. Results and Discussion

Analysis of the XRD results for the non-stoichiometric powders indicate that the two sets of powders obtained were very similar for both processing routes as was expected. However, a detailed examination shows that the microstructural and physical properties of the tracks are sensitive to varying amounts of excess Ba and Cu cations. The XRD results obtained from the surfaces of fired films reveal the predominance of 123 within the tracks with varying degrees of texture and varying amounts of secondary phases at the different compositions.

Despite the similarity of the two powders of composition A the subsequently fired tracks were very different. In track A(2) large extended 123 spherulites cover the surface of the track up to a maximum diameter of approximately 5mm, thus spreading across the whole width of the track. These spherulites are discrete structures, separated on the surface from neighbouring spherulites by secondary phases including 211 (Fig. 2). It was also noted that some regions within the spherulites contained particularly heavily twinned 123 platelets, which appear to 'decorate' these spherulites. This was in contrast to the spherulitic surface morphology observed in the YBCO control track where individual spherulites had a maximum diameter of only approximately 0.6mm, and no similarly 'decorated' areas could be recognised.

The surface microstructure in track A(1) was seen to be comparable to the control, again exhibiting small discrete spherulites, but like A(2) small platelets of 123 were again apparent.

With increasing flux content, i.e. in tracks of compositions B and C, the surface morphology progressively deviated away from the spherulitic-type structure. In both B(1) and B(2) the basic 123 spherulitic structures could still be identified but these were no longer individual discrete structures, but instead neighbouring spherulites coalesced with no secondary phases evident to separate them (Fig. 3). Within this structure there is also an increased quantity of large highly twinned platelets of 123 at the surface. At composition C, in both C(1) and C(2) there remains little evidence of the

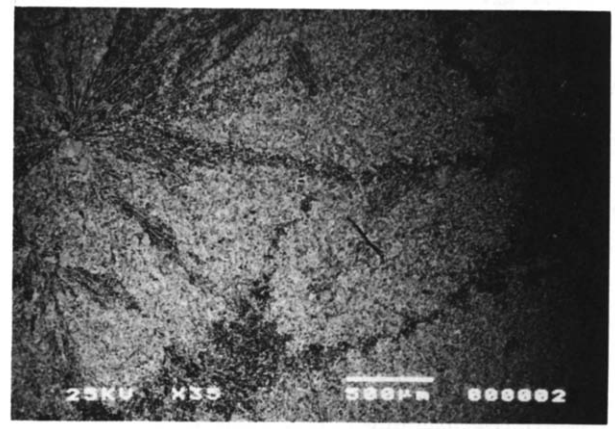

Fig. 2 The large spherulites observed on the surface in track A(2)

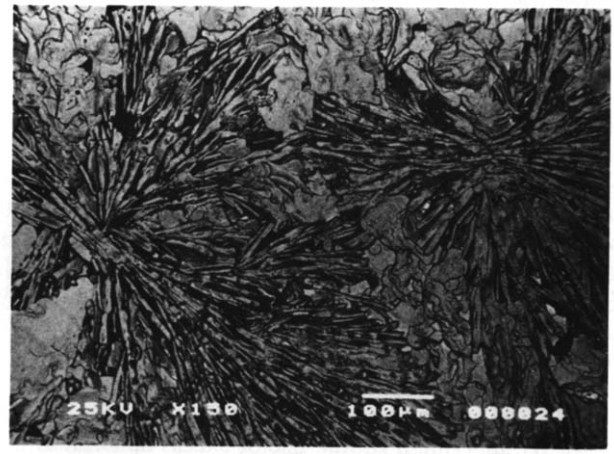

Fig. 3 The coalescence of spherulites found on the surface in tracks of composition B

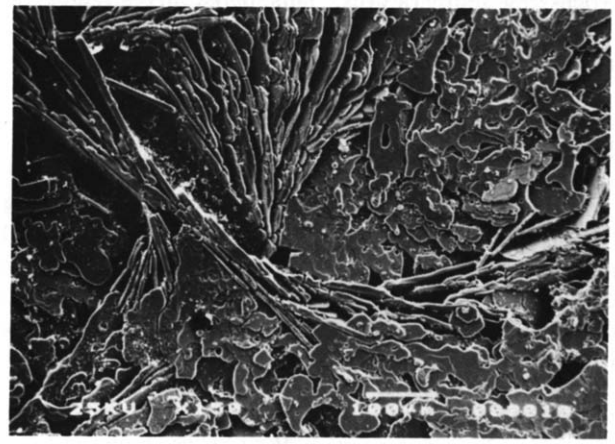

Fig. 4 Platelets of 123 found on the surface in tracks of composition C

existence of spherulitic morphology. Most of the surface consists of highly twinned platelets of 123 which are typically larger than the platelets seen in the tracks of composition A and B. These platelets predominantly lie with their c-axis perpendicular to the plane of the track, but as seen in Fig. 4 there are areas where the c-axis of the platelets rotate to lie in the plane of the track. These appear to be analogous to the features at the centres of individual spherulites in the control, A and B tracks.

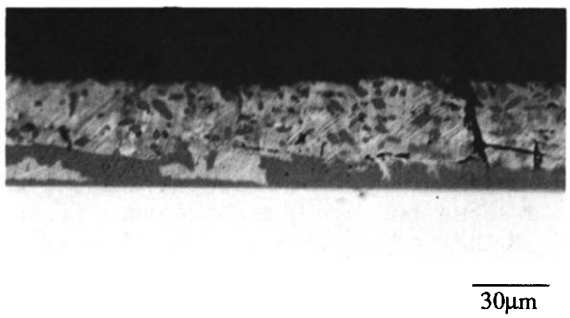

Fig. 5 Cross-sectional micrograph of the control YBCO track.

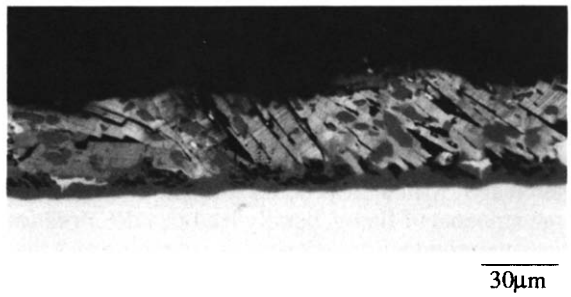

Fig. 6 Cross-sectional micrograph of track (A2)

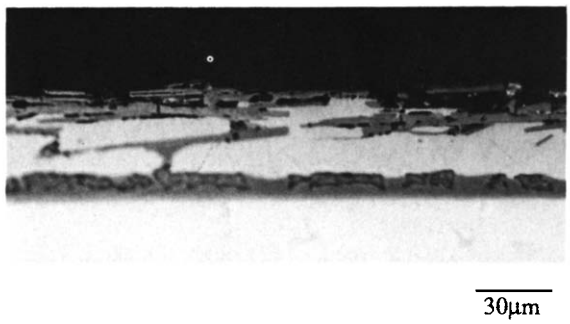

Fig. 7 Cross-sectional micrograph of track (C1)

Comparison between the cross-sections shown in Figs. 5-7 show that the nature of the reaction layer between the substrate and the film has been significantly changed in tracks with flux additions. It is apparent that with both the 32.4% and the 64.7% flux additions the tracks show increasing quantities of secondary phases, evident within this zone, to such an extent in C that these secondary phases occupy the majority of the tracks (Fig. 7). EDX analysis showed that these phases consist of BaCuO2 andCuO (consistent with the XRD results) and a substrate reaction layer of $Ba(Zr_{1-x}Cu_x)O_y$. The details of this analysis will be reported at a later date. In the control YBCO track there is a dispersion of a large number of fine 211 particles throughout the 123 matrix phase (Fig. 5). In A(1) and A(2) the 211 particles are much larger, but fewer in number than those evident in the control (Fig. 6). In tracks B(1) and B(2) the overall proportion of 211 is significantly less, there being fewer and smaller particles apparent, whilst in tracks C(1) and C(2) there is virtually no 211 remaining at all (Fig. 7).

It can also be seen from the cross sections that in all the non-stoichiometric tracks the 123 appears to grow in the form of laths (or platelets, as was also apparent from the surface micrographs). This is more obvious with increasing quantities of flux additions, and is most clearly shown in Fig. 7 where a thin layer of 123 platelets can be seen at the surface of the track, (C1).

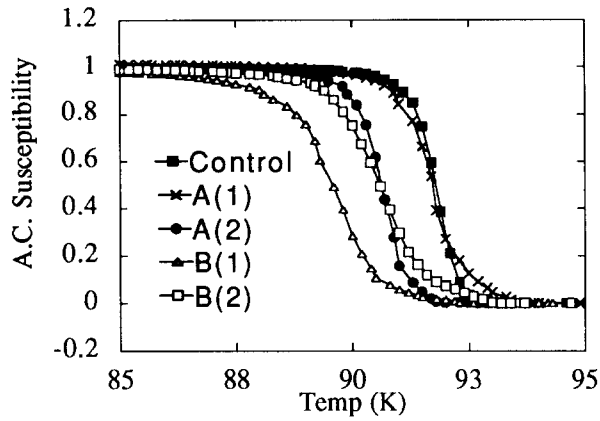

Fig. 8 A.C. susceptibility traces for tracks showing sharp magnetic transitions

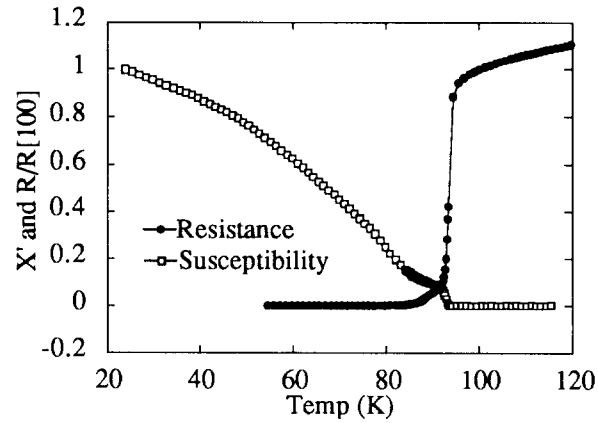

Fig. 9 The A.C. susceptibility and resistive transitions for track C(1)

The A.C. susceptibility traces in Fig. 8 show that the control track and the tracks of compositions A, B show

sharp transitions within approximately 3K of each other. However, the 64.7% flux addition caused the magnetic transition to degrade as shown in Fig. 9, but as also shown in this figure the track still gives a sharp resistive transition.

A four point probe method was used to measure the current carrying capacity at 77K for each of the tracks.

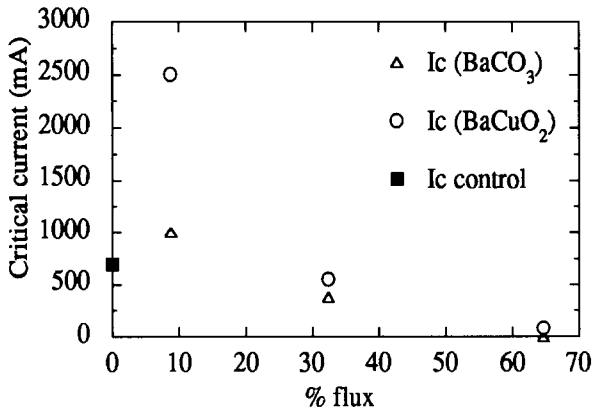

Fig. 10 Graph of critical current measurements for the non-stoichiometric tracks, showing them as a comparison with the control track

As shown in Fig. 10 an 8.8% flux addition produces an initial improvement in Ic, which is then reduced with further flux additions. Most of these results can be related to the relative proportions of 123 material in the respective tracks. At compositions B and C there are increasing quantities of the secondary phases CuO and $BaCuO_2$ present in the tracks, as was shown in the cross sections (Figs. 5-7). Consequently there is less superconducting material available to support the passage of current and as such there is a decrease in the critical current values. Conversely, the reaction layer was reduced in A(1) and A(2) tracks, resulting in a greater proportion of 123 which correlates to the higher critical current carrying performances. However Fig. 8 shows that there is a considerable difference between the performance of A(1) and A(2). Microstructural observations indicated that the essential difference between A(1) and A(2) was the dramatic difference in the size of their respective spherulites. This implies that spherulites play an important role in the current carrying ability of thick films and indicates that the spherulite size is of particular importance. This however, must also be related to the quality of the grain boundaries, and the interconnectivity between grains and is also dependent on the secondary phases present in these regions.

Ruckenstein et al. [8] have performed a series of experiments investigating the kinetics of the reactions between the possible constituent oxides of YBCO. Their results show that reactions involving $BaCuO_2$ are very rapid, but those involving $BaCO_3$ are limited. Initially $BaCO_3$ reacts quickly but then the reaction rate significantly slows down to such an extent that unreacted $BaCO_3$ will always remain unless lengthy extended calcining times are employed.

In the precursor powders of compositions B(1&2) and C(1&2) large amounts of flux have been added. In B(1) and C(1) the $BaCO_3$ will have been slow to react and some $BaCO_3$ will remain unreacted. However this residual material will be insignificant compared to that greater proportion of flux which will have reacted. So these powders will essentially be the same at each composition, which ever route (1 or 2) was used. This may not be true with powders A(1&2). At this composition only a small proportion of flux has been added, so that residual unreacted $BaCO_3$ will be more significant. This implies that powders A(1) and A(2) may have a subtle but significant difference in their $BaCO_3/BaCuO_2$ content. In turn, this may be responsible for the dramatic different in surface morphology of these two tracks and the correponding difference in critical current capacity.

4. Conclusions

It has been shown that the addition of a small amount of Ba/CuO flux can significantly influence the surface morphology and improve the critical transport current measured at 77K in melt-processed films. The additions of large amounts of flux generally lead to a deterioration of the superconducting properties in melt-processed YBCO films. The distribution and size of the 211 inclusions is also significantly affected by flux additions.

Acknowledgements

To John Knight for assistance in polishing cross sections of the thick films.

References

1. M.J. Day , F. Wellhofer, T. C. Shields, J. S. Abell Physica C 185-189, 2395 (1991)
2. M.S. Colclough, J. S. Abell, C. E. Gough, J. Rickets, T. C. Shields, F. Wellhofer, W. F. Vinen, N. McN. Alford, T. Button Cryogenics 29, 439-444 (1991)
3. J.S. Abell, T. C. Shields, F. Wellhofer, K. N. R. Talylor, D. Holland Physica C 162-164, 1265 (1989)
4. D. L. Kaiser, F. Holtzberg, B. A. Scott and T. R.McGuire. Appl. Phys. Lett. 51, 1040, (1987)
5. L. F. Schneemeyer, J. W. Wasczac, T. Siegrist, R. B. vanDover, L. W. Rupp, B. Batlogg, R. J. Cava and D. W. Murphy Nature 328, 601 (1987)
6. .A. Drake, J. S. Abell and S. Sutton J. Less Common Metals 164-165, 187(1990)
7. T. Aselage and K. Keefer J. Mater. Res. 36, 1279 - 1291 (1988)
8. E. Ruckenstein, S. Narain, N.-L.Wu, J. Mater. Res. 4, 2, 267 (1989)